Development 134, 1385-1395 (2007) doi:10.1242/dev.02816

The nuclear envelope protein MAN1 regulates TGFβ signaling and vasculogenesis in the embryonic yolk sac

Tatiana V. Cohen, Ourania Kosti and Colin L. Stewart*

MAN1 is an integral protein of the inner nuclear membrane of the nuclear envelope (NE). MAN1 interacts with SMAD transcription factors, which in turn are regulated by the Transforming growth factor beta (TGFβ) superfamily of signaling molecules. To determine the role of MAN1 in mouse development, we used a gene-trap embryonic stem cell clone to derive mice with a functional mutation in MAN1 (*Man1*$^{GT/GT}$). Expression of *Man1* during early development is initially low but increases at embryonic day 9.5 (E9.5). Coincident with this increase, homozygous gene-trapped *Man1* (*Man1*$^{GT/GT}$) embryos die by E10.5. Examination of mutant embryos and tetraploid rescue experiments reveals that abnormal yolk-sac vascularization is the probable cause of lethality. We also established embryonic stem cell lines and their differentiated derivatives that are homozygous for the *Man1*^{GT} allele. Using these lines, we show that the *Man1*^{GT} allele results in increased phosphorylation, nuclear localization and elevated levels of SMAD transcriptional activity, predominantly of SMAD2/3, which are regulated by the ALK5 signaling pathway. Our studies identify a previously uncharacterized role for an integral nuclear envelope protein in the regulation of yolk-sac angiogenesis by TGFβ signaling and reveal that the NE has an essential role in regulating transcription factor activity during mouse development.

KEY WORDS: Nuclear envelope, Vasculogenesis, *Man1* (*Lemd3*), TGFβ

INTRODUCTION

The nucleus of mammalian cells is bounded by the nuclear envelope (NE) and underlying nuclear lamina. The NE consists of an inner nuclear membrane (INM) and outer nuclear membrane (ONM). The two membranes are contiguous, being linked at the periphery of each nuclear pore complex. The nuclear lamina, which underlies the INM, primarily consists of the nuclear intermediate filament proteins, the A- and B-type lamins (Burke and Stewart, 2002). A growing body of evidence suggests that the lamins, as well as other proteins associated with the lamina and nuclear envelope, are crucial for interphase nuclear architecture, the structural integrity of the nucleus, gene regulation, DNA replication and chromatin organization. These activities are also highlighted by the fact that at least nine different diseases, ranging from muscular dystrophy to premature aging (the laminopathies), are linked to mutations within the lamin A gene (Burke and Stewart, 2002). In addition to the laminopathies, other diseases are caused by mutations in proteins associated with the NE (Gruenbaum et al., 2005; Worman, 2005).

Some eighty different NE-associated proteins have been identified (Schirmer et al., 2003), and among these are members of the LEM domain family (Lee and Wilson, 2004; Schirmer et al., 2003). LEM domain proteins contain a 43 amino acid motif facing the nucleoplasm, shared by the prototype members of the LEM family, LAP2, emerin and MAN1 (LEMD3) (Cai et al., 2001; Laguri et al., 2001; Lin et al., 2000; Wolff et al., 2001). Although mutated forms of emerin and possibly LAP2 result in muscular dystrophy and cardiomyopathy (Melcon et al., 2006; Morris, 2004; Taylor et al., 2005), the functions of LEM domain proteins are still ill-defined. In *Xenopus*, XMAN1/SANE functions as an embryonic neuralizing factor, by antagonizing bone morphogenetic protein (BMP) signaling (Osada et al., 2003; Raju et al., 2003), whereas in humans, mutations in *MAN1* (*LEMD3*) result in bone and connective tissue disorders (Hellemans et al., 2006; Hellemans et al., 2004).

TGFβ/BMP/activin signaling pathways activate SMAD transcription factors and are important in regulating mouse embryogenesis (Goumans and Mummery, 2000). Previous studies revealed that MAN1 binds to and regulates SMAD transcriptional activity, suggesting a potentially significant role for MAN1 in regulating TGFβ/BMP signaling (Hellemans et al., 2004; Lin et al., 2005; Pan et al., 2005). To determine the role of *Man1*, we analyzed the expression of *Man1* and used a gene-trapped (GT) embryonic stem (ES) cell clone to derive mice with a functional mutation in the *Man1* gene. We show that *Man1* is essential for embryonic vasculogenesis and that the *Man1*$^{GT/GT}$ mutation results in hyperactivation of some components in TGFβ signaling pathways.

MATERIALS AND METHODS

Generation of *Man1*$^{GT/GT}$ mice

The ES cell line XST167, containing a gene-trap insertion mutation (Skarnes, 1990) in the *Man1* locus (BayGenomics, San Francisco, CA), was microinjected into C57Bl/6 blastocysts as described (Stewart, 1993). The resulting *Man1*^{GT} line was maintained as heterozygotes and intercrossed to obtain homozygotes (*Man1*$^{GT/GT}$). All mice were maintained in our facility in accordance with the procedures outlined in the Guide for the Care and Use of Laboratory Animals (NIH Publication No. 86-23, 1985).

Genotypes were determined by Southern blotting or RT-PCR. For Southern analysis, a 300 bp genomic fragment, generated using primers 5′-GCGCTGGGTTACTTTGTGTGCTG-3′ and 5′-GCTTCCCGTTCA-CCACACTTCTG-3′, was used to probe DNA digested with *Eco*RV. Embryos were genotyped by RT-PCR using forward primer 1 located within exon 4 (5′-GACCATGAATGTGGCAGTTCTA-3′) and reverse primer 2 located within exon 5 (5′-CGTACATGTGGAATAGGCATGTAAGG-3′) to obtain a 424 bp wild-type PCR product and primer 1 and reverse primer 3 located within the β-geo sequence (5′-TCGTCTGCTCATCCATGACC-3′) to obtain a 1.6 kb mutant PCR product.

Cancer and Developmental Biology Laboratory, National Cancer Institute, Frederick MD 21702, USA.

*Author for correspondence (e-mail: stewartc@ncifcrf.gov)

Accepted 9 January 2007

Northern analysis
Total RNA was extracted using the RNeasy Kit (Qiagen, Valencia, CA). Ten micrograms of RNA were separated on 1% formaldehyde 1% agarose gels and transferred to Hybond membranes (Amersham Biotech, Piscataway, NJ). The mouse cDNA corresponding to nucleotides 1261-1898 bp of the *Man1* transcript (I.M.A.G.E. Consortium clone ID 455955) was used as a probe and a *Gapdh* cDNA as a loading control. Tissue and embryonic blots were obtained from Seegene (Rockville, MD).

Derivation of *Man1*$^{GT/GT}$ gene-trapped cells
Blastocysts from *Man1* heterozygous intercrosses were used to derive homozygous *Man1*$^{GT/GT}$ ES cells as described (Abbondanzo et al., 1993; Stewart et al., 1995). ES clones were genotyped by northern analysis (see above). Embryoid bodies (EBs) were prepared by growing ES cells in suspension. Two-week-old EBs were plated onto 35 mm culture dishes to allow formation of explants.

Homozygous *Man1*$^{GT/GT}$ embryonic stem cells were injected into blastocysts and *Man1*$^{GT/GT}$ fibroblasts were derived from chimeric embryos at embryonic day 13 (E13) as described (Escalante-Alcalde et al., 2003). *Man1*$^{GT/+}$ and wild-type fibroblasts were derived from embryos of heterozygous crosses as described (Escalante-Alcalde et al., 2003). Primary fibroblasts were immortalized by retroviral infection with SV40 large T antigen (Zhu et al., 1991). For SMAD translocation experiments, PMEFs were infected with retroviral vector (pBabe-Puro) containing a full-length MAN1 cDNA tagged with a Flag epitope (kind gift of Howard Worman, Columbia University, New York, NY).

Tetraploid rescue
Wild-type tetraploid embryos were prepared by incubating fertilized (C57Bl/6×C3H F1) oocytes overnight in KSOM (Specialty Media) with 0.25 μg/ml cytochalasin D (Sigma), which suppresses the first cleavage division, making the zygotes tetraploid. The embryos were washed four times in KSOM to remove the cytochalasin D and allowed to progress to the two-cell stage. Two-cell-stage embryos were transferred to the oviducts of pseudopregnant recipients for an additional 24-48 hours for further development. Tetraploid blastocysts were recovered and injected with *Man1*$^{GT/GT}$ ES cells. Embryos were transferred to pseudopregnant B6CBAF1 recipients with the embryos being recovered on E9.5-12.

Histological staining
Embryos aged E8.0-10.0 were stained for *lacZ* expression and photographed as previously described (Escalante-Alcalde et al., 2003). Benzidine staining to detect blood islands was performed as described (Orkin et al., 1975).

Embryos were whole-mount immunostained with antibodies to platelet endothelial cell adhesion molecule (PECAM-1; also known as PECAM1) and FLK-1 (KDR – Mouse Genome Informatics) (BD Biosciences, San Diego, CA), as described (Byrd et al., 2002; Schlaeger et al., 1995). For immunohistochemistry, embryos were fixed in 4% paraformaldehyde, embedded in paraffin, sectioned and stained using indicated antibodies. Immunofluorescence using an antibody to fibronectin was performed as described (Zwijsen et al., 1999).

EB explants were immunostained with PECAM-1 as described (Escalante-Alcalde et al., 2003). For fluorescence activated cell sorting (FACS) analysis to quantify expression of PECAM-1 in EB explants, 7-day-old explants were trypsinized, immunostained with an antibody to PECAM-1 conjugated to phycoerythrin (PE, BD Biosciences) and analyzed on an LSR1 flow cytometer using CellQuest software (Becton Dickinson). Unstained cultures were used as negative controls.

Immunofluorescence
Mouse embryonic fibroblasts (MEFs) were fixed with 4% paraformaldehyde, stained with primary antibodies to SMAD1 (Santa Cruz, CA), SMAD2/3 (BD Biosciences) and Flag (Affinity Bioreagents, Golden, CO) and then with secondary antibodies conjugated to Alexa 488 or Alexa 568 (Molecular Probes, Eugene, OR). After immunolabeling, coverslips were mounted in Vectashield Mounting Medium (Vector Laboratories, Burlingame, CA) and visualized using a Zeiss Axiophot inverted microscope.

Western analysis
Whole cell lysates of MEFs were immunoblotted with a rabbit polyclonal antiserum raised against a peptide (aa898-911) at the C-terminus of MAN1. Antibodies used were for fibronectin (1:300, ICN), p21 (1:100, BD Pharmingen), SMAD2 (1:250, Zymed, San Francisco, CA), pSMAD2 (1:250, Upstate, Charlottesville, VA), pSMAD1 (Cell Signaling, St Louis, MO), and actin (1:1000, Santa Cruz). Detection was performed using Chemiluminescence Reagent Plus (PerkinElmer, Boston, MA). Cytoplasmic and nuclear fractions were prepared using the NE-PER kit (Pierce, Rockford, IL) according to the manufacturer's instructions.

Transient transfection and luciferase reporter assays
The pTP3-Lux construct containing a TGFβ1-responsive Plasminogen Activated Inhibitor I (PAI-1) promoter linked to a luciferase cDNA (Wrana, 2000) (a kind gift of Joan Massague, Memorial Sloan-Kettering Cancer Center, New York, NY) was transfected into MEFs using Fugene 6 (Roche, Indianapolis, IN) according to the manufacturer's instructions. To normalize for transfection efficiency, cells were co-transfected with 0.5 μg pTK-RL (Promega, Madison, WI). After 42 hours following the transfection, cultures were incubated for 8 hours with hrTGFβ1 (R&D Systems) at indicated concentrations. Luciferase activities were measured using the Dual-Luciferase Assay according to the manufacturer's instructions (Promega).

Cell proliferation assay
MEFs were seeded onto 96-well culture dishes at a concentration of 5×10^3 cells per well and treated with indicated concentrations of hTGFβ1 (R&D Systems). The endothelial cell line SVEC (ATCC #CRL-2181) was previously characterized (O'Connell and Edidin, 1990). After 48 hours, cells were incubated overnight with MTT using the Cell Proliferation Kit I (Roche) according to the manufacturer's instructions. Quantification of the formazan reaction product in active cells was performed using the VersaMax Plate reader (Molecular Devices).

Real-time analysis
RNA from MEFs and EB explants was extracted using the RNeasy Kit and 1 μg was reverse-transcribed using the First-Strand cDNA Synthesis Kit (Roche). Real-time PCR was performed on an ABI Prism 7000 using SYBR Green Master Mix (AB, Warrington, UK).

RESULTS
Generation of mutant mice
To determine the function of *Man1* during development, we used an ES cell line containing a gene-trap insertion into the *Man1* locus. The gene-trap insertion, mapped by Southern analysis (Fig. 1A,B), introduces a novel *en2* splice acceptor site and a β-galactosidase (β-gal) cDNA linked to the neomycin resistance cDNA (*β-geo*) within the *Man1* intron between exon 4 and 5 (Skarnes, 1990). Northern analysis of RNA from heterozygous fibroblasts revealed a 7.7 kb *Man1-β-geo* hybrid transcript in addition to the wild-type 4.7 kb transcript (Fig. 1C), indicating that the *β-geo* sequence is in frame with the *Man1* transcript and the first 1702 bp of the endogenous *Man1* transcript is retained. No additional transcripts were observed, indicating additional alternative splicing to exons downstream of the gene-trap insertion into *Man1* did not occur. This analysis predicts that the gene-trapped *Man1*^{GT} allele produces a fusion protein consisting of 567 N-terminal MAN1 amino acids fused to β-geo and lacking the C-terminal sequence downstream of exon 4 (Fig. 1D). Western analysis using an antibody derived from the C-terminus of MAN1 confirmed that the C-terminus was no longer recognized (Fig. 1E).

Man1 expression during embryogenesis
The expression of *Man1* was initially determined by northern analysis (not shown). In embryonic tissues, the signal intensity of *Man1* was low at stages E4.5 through E8.5 and increased in intensity in later developmental stages from days E9.5 through E18.5. Low

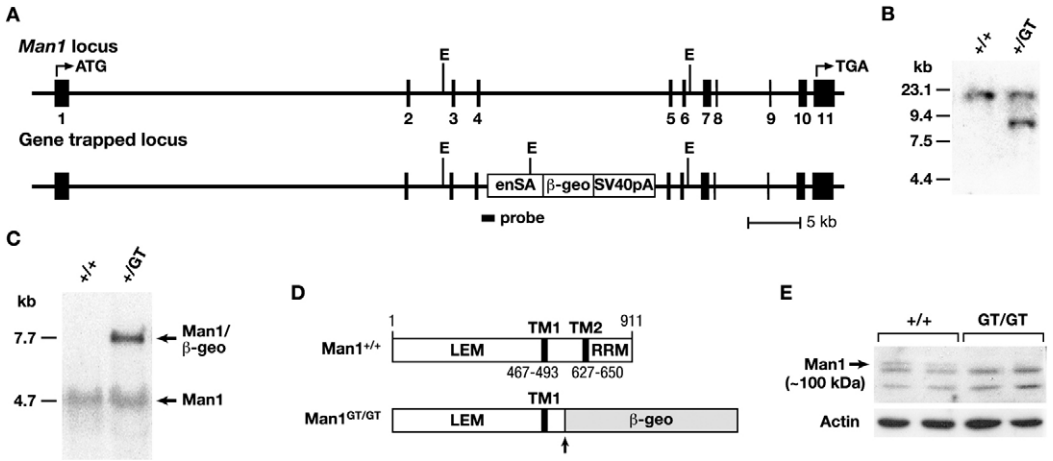

Fig. 1. Mapping the gene-trap insertion in the *Man1* locus. (**A**) Upper panel: the *Man1* gene, showing exon organization (black boxes). Lower panel: the gene-trap vector, containing the *engrailed2* intron (en2) and splice acceptor (SA), a β-galactosidase-neomycin fusion cDNA (β-geo), an SV40 polyadenylation site (SV40pA) integrated between exons 4 and 5. 'Probe' indicates the location of the genomic probe used in Southern blotting. (**B**) Southern blot of genomic DNA from gene-trapped mice. Approximate size of detected DNA is indicated. (**C**) Northern blot, demonstrating 4.7 kb endogenous and 7.7 kb *Man1/β-geo* transcripts in wild-type (+/+) or heterozygous (+/GT) MEFs. (**D**) The MAN1 911 amino acid polypeptide contains the LEM domain at the N-terminus, the RRM domain at the C-terminus and two transmembrane domains. The gene-trap insertion product retains the 567 N-terminal amino acids (arrow) linked to β-galactosidase. (**E**) Western analysis on MEF whole cell extracts using an antibody raised to a C-terminus peptide shows that the C-terminus of MAN1 is absent in homozygotes (GT/GT). +/+, wild-type; +/GT, heterozygote; E, *Eco*RV.

levels of the *Man1* transcript were also observed in most adult tissues, whereas robust expression was seen in the brain, testes and placenta. We used the β-galactosidase activity of the gene-trapped fusion protein product to further determine the expression of *Man1* during development. Expression of $Man1^{GT}$ was first detectable in the ectoplacental cone and yolk sac at E8.5 (Fig. 2A). At E9.5, *lacZ* expression increased initially in the gut epithelium and the floor plate (Fig. 2B) and by E11 spread to the skin and throughout the embryo (Fig. 2C), consistent with the widespread expression of *Man1* detected by northern analysis. At E13, expression was widespread, with robust staining observed in the central nervous system (Fig. 2E-G), including the midbrain and hindbrain, neural tube, pons and cerebellum. Staining was also observed in the placenta (Fig. 2D,E) and yolk sac (Fig. 2E,H,I) in the visceral endoderm, endothelial cells and mesoderm but excluded from blood cells (Fig. 2H,I).

Gene-trapping *Man1* results in embryonic lethality

Intercrossing *Man1* heterozygotes produced offspring, of which 38% were wild type, 62% were heterozygotes and none were homozygotes ($Man1^{GT/GT}$) (Table 1). Examination of embryos at various stages from *Man1* heterozygous intercrosses revealed that $Man1^{GT/GT}$ embryos were indistinguishable from wild-type embryos up to E8.5 (data not shown). By E9.5, the $Man1^{GT/GT}$ embryos were smaller and developmentally delayed (Fig. 3A,B), did not undergo axial rotation and had an abnormally developed heart with an enlarged pericardium (Fig. 3A,B). Expression of *lacZ* in the $Man1^{GT/GT}$ embryos at E9.5 was restricted to the yolk sac, allantois and amnion (Fig. 3C). By E10.5, $Man1^{GT/GT}$ embryos had ceased growing, with the yolk sac being expanded and the pericardium enlarged and edematous (Fig. 3D). In the $Man1^{GT/GT}$ yolk sacs, the cell layers were highly disorganized, with *lacZ* expression being restricted to the endoderm, endothelium and mesoderm but not blood cells (Fig. 3E). Closer examination of individual cells revealed β-gal staining was predominantly localized to the nuclear envelope, and to a lesser degree to the nucleus and cytoplasm, indicating that the targeting of MAN1-β-gal to the NE is apparently unaffected by the gene-trap mutation (Fig. 2F). Some β-gal staining was also observed in the endoplasmic reticulum, which is contiguous with the nuclear envelope.

Lethality in $Man1^{GT/GT}$ embryos is due to defective vasculogenesis

The first site of vasculogenesis is the embryonic yolk sac. The yolk sacs of $Man1^{GT/GT}$ embryos were distinctly different from wild-type embryos (Fig. 4). Wild-type yolk sacs contained large branching vessels and a capillary network. $Man1^{GT/GT}$ yolk sacs were completely devoid of large blood vessels, and the blood vessels remained as a primitive capillary plexus, interspersed with blood pools (Fig. 4A). The presence of erythrocytes in $Man1^{GT/GT}$ embryos was confirmed by benzidine staining (Fig. 4B). Immunostaining for the endothelial marker PECAM-1 in $Man1^{GT/GT}$ yolk sacs demonstrated the presence of endothelial cells along primitive capillary networks, indicating that vasculogenesis had commenced

Table 1. Analysis of progeny from heterozygous ($Man1^{GT/+}$) intercrosses

	Genotype					
Age	+/+	GT/+	GT/GT	Total	χ^2	*P*
3 weeks postpartum	44 (29)	71 (57)	0 (29)	115	39.99	<0.001 (2 *df*)
Embryo (at E9.5)	18 (17)	31 (33)	18 (17)	67	0.239	Not significant

Observed numbers of progeny of each genotype are indicated and expected numbers, based on mendelian ratio 1:2:1, are in parentheses.

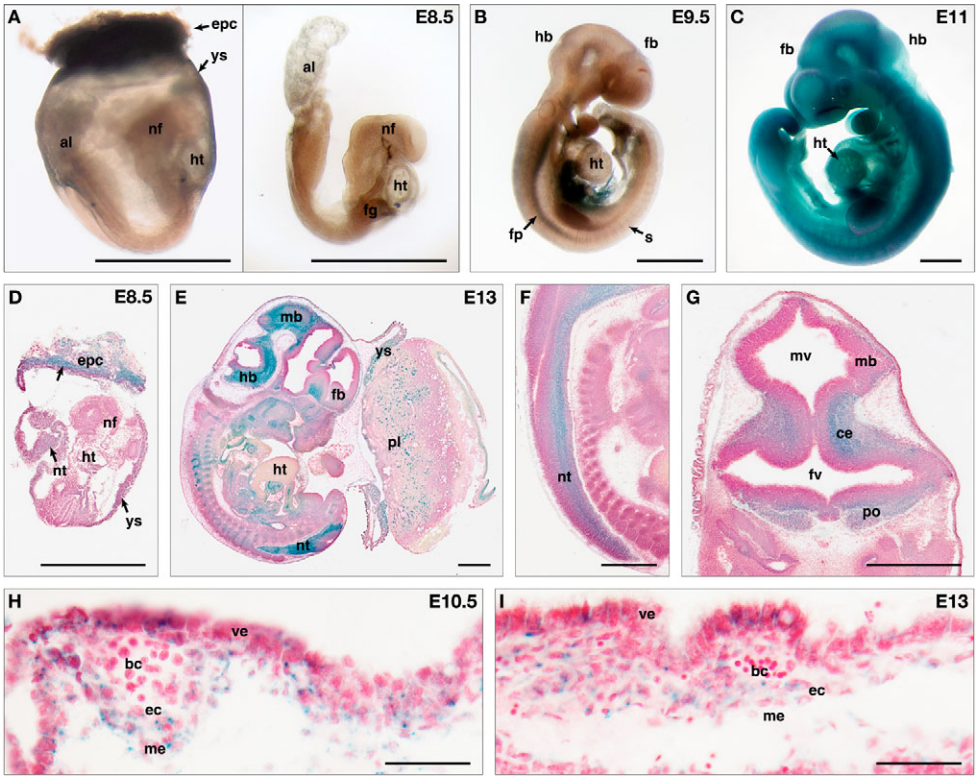

Fig. 2. Expression of the *Man1-lacZ* reporter in embryos. (**A-C**) Whole-mount *lacZ* staining in heterozygotes at stages E8.5-11. (**D-F**) Sagittal sections showing expression of *Man1-lacZ* in both embryonic and extraembryonic compartments. (**G**) Frontal section showing expression of *Man1-lacZ* in the CNS. (**H**,**I**) High magnification views of sections through the yolk sac. Scale bars: 1 mm in A-G; 0.05 mm in H,I. al, allantois; bc, blood cells; ce, cerebellum; ec, endothelial cells; epc, ectoplacental cone; fb, forebrain; fg, foregut; fp, floor plate; fv, fourth vesicle; hb, hindbrain; ht, heart; mb, midbrain; me, mesothelium; mv, medial vesicle; nf, neural fold; nt, neural tube; pl, placenta; po, pons; s, somites; ve, visceral endoderm; ys, yolk sac.

(Fig. 4C). Although the allantois frequently fused with the chorion in *Man1*$^{GT/GT}$ embryos, it often was structurally abnormal (data not shown).

Vasculogenesis was also defective in *Man1*$^{GT/GT}$ embryos proper. The embryonic vasculature was visualized by staining with antibodies to the VEGF receptor FLK-1. Well-formed vascular networks were observed in wild-type embryos (Fig. 4D). By contrast, development of the *Man1*$^{GT/GT}$ embryos was delayed some 24-36 hours, with the vasculature of *Man1*$^{GT/GT}$ embryos being highly disorganized (Fig. 4E,F). These observations suggest that, whereas the initiation of vasculogenesis proceeds in *Man1*$^{GT/GT}$ embryos, formation of large blood vessels and angiogenesis are perturbed.

The yolk-sac abnormality in *Man1*$^{GT/GT}$ mice is not due to defective placental function

Abnormal development and lethality of embryos around E8.5-9.5 is frequently due to primary defects in placental development (Rossant and Cross, 2001). To establish whether the *Man1*$^{GT/GT}$ phenotype was due to placental defects, we performed a tetraploid rescue experiment. Diploid *Man1*$^{GT/GT}$ ES cells were microinjected into wild-type tetraploid blastocysts and transferred to pseudopregnant recipients. Postimplantation embryos were recovered on E9.5 or E12. Of the 36 blastocysts transferred, three embryos were found to resemble the *Man1*$^{GT/GT}$ phenotype (Table 2), and their genotype was confirmed by RT-PCR. Of these three, two were delayed approximately 36 hours and blood vessels had not formed from the primitive plexus. The third embryo contained irregularly shaped blood vessels and had undergone embryonic axial rotation but was edematous and small compared to E9.5 wild-type embryos. No embryos were observed to develop beyond the *Man1*$^{GT/GT}$ phenotype and none were recovered at E12. As the wild-type tetraploid cells form the placenta and visceral endoderm layer of the yolk sac, our results indicate that embryonic lethality was probably not due to a defect in placental function.

Table 2. Summary of tetraploid rescue experiments

No. injected	No. recovered at E9.5	Approximate time of death			Live
		Resorbed	E8.0	E9.5	
36	21	18	2	1	0

Disorganized vasculogenesis in *Man1*$^{GT/GT}$ yolk sacs

Differentiation and formation of the vascular endothelium occurs in the yolk-sac mesoderm (Baron, 2003). In wild-type yolk sacs, the endoderm and mesoderm are tightly apposed and contain many developing blood vessels and discreet blood islands (Fig. 5A). In *Man1*$^{GT/GT}$ yolk sacs, the endoderm and mesoderm were poorly attached to each other, resulting in large lacunae containing blood cells (Fig. 5B). Immunostaining with antibodies to PECAM-1 and FLK-1 revealed that although endothelial cells were present in *Man1*$^{GT/GT}$ yolk sacs, many remained rounded, were misaligned or had failed to incorporate into the vessel walls (Fig. 5B,C).

Formation of branched blood vessels during vasculogenesis requires the proliferation and recruitment of smooth muscle cells to line the vessel walls. TGFβ1 is a potent inhibitor of vascular smooth muscle cell (VSMC) proliferation (Feinberg et al., 2004). We analyzed sections immunostained with an antibody for the VSMC marker α-smooth muscle actin (ACTA2) (Fig. 5D). Yolk sacs from wild-type embryos contained a large number of VSMCs, whereas VSMCs appeared to be less abundant in the *Man1*$^{GT/GT}$ embryos. Quantification of *Acta2* transcripts in E9.5 yolk sacs by RT-PCR revealed an approximately twofold reduction in transcript levels in the *Man1*$^{GT/GT}$ yolk sacs compared with wild type (data not shown). This reduction in VSMCs is probably due to their decreased

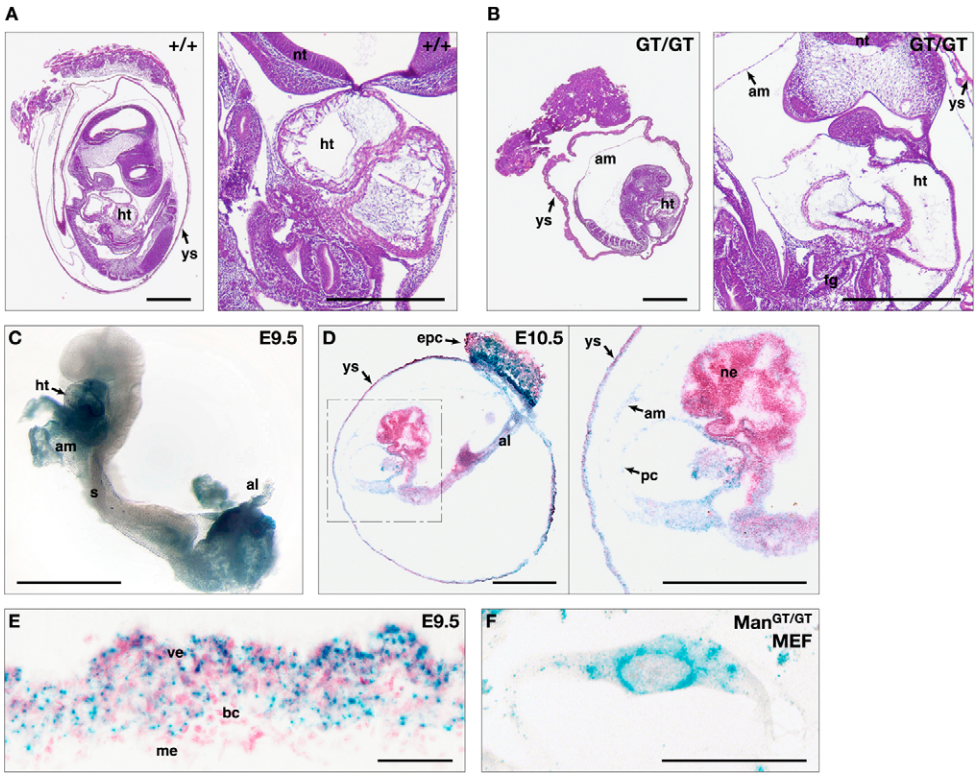

Fig. 3. Morphological analysis of *Man1*$^{GT/GT}$ embryos. (**A**,**B**) Sagittal sections of wild-type (+/+) and *Man1*$^{GT/GT}$ (GT/GT) E9.5 embryos stained with H&E. Left panels are low magnification views of sagittal sections. Right panels are high magnification views of frontal sections showing overall growth retardation and abnormal cardiac development in the *Man1*$^{GT/GT}$ embryos. (**C**) *Man1*$^{GT/GT}$ E9.5 embryo stained for *lacZ* expression with strong expression in the heart, amnion and allantois. (**D**) Sagittal section of an *Man1*$^{GT/GT}$ E10.5 embryo stained for *lacZ* expression. Inset is at higher magnification. (**E**) Yolk-sac section of *Man1*$^{GT/GT}$ E9.5 embryo shows disruption in the endodermal and mesodermal layers. (**F**) *lacZ* staining in cultured *Man1*$^{GT/GT}$ MEFs, showing strong localization to the nuclear envelope. Scale bars: 1 mm in A-E; 50 μm in E,F. ne, neuroectoderm.

proliferation and defective recruitment into developing blood vessels, resulting in the subsequent failure of nascent capillaries to form functional blood vessels.

Reduced proliferation of *Man1*$^{GT/GT}$ endothelial cells

The vascular defects in the *Man1*$^{GT/GT}$ embryos may be due to defective differentiation, proliferation or organization of the endothelial cells (ECs) to form the primitive capillaries. To characterize these defects, we generated embryoid bodies (EBs) from wild-type and *Man1*$^{GT/GT}$ ES cells. EBs cultured in suspension for 2 weeks were re-plated and formed explants containing a large number of PECAM-1$^+$ ECs (Fig. 6A,B). The explants of both *Man1*$^{GT/GT}$ and wild-type EBs contained PECAM-1$^+$ cells arranged in capillary networks, indicating that *Man1*$^{GT/GT}$ ECs can differentiate from precursors and form capillaries. However, the capillary networks in the *Man1*$^{GT/GT}$ explants were less expansive and were surrounded by many PECAM-1$^+$ cells that had not integrated into the vascular network (Fig. 6B). Formation of branched blood vessels from primitive capillaries requires endothelial cell proliferation and organization to form the vessel lumen (Risau and Flamme, 1995). Thus, despite the formation of ECs in *Man1*$^{GT/GT}$ embryos and EBs, further organization into branched structures is defective. Quantitation of PECAM-1$^+$ ECs in the EB explants was performed using FACS analysis. During differentiation, ECs first express low levels of PECAM-1, then expression of PECAM-1 increases as ECs differentiate from precursors (Levenberg et al., 2002). In accordance, two peaks of PECAM-1$^+$ cells were observed by FACS analysis. No difference was observed between wild-type and *Man1*$^{GT/GT}$ cultures in the fraction of low-expressing PECAM-1$^+$ precursor cells, while the fraction of high PECAM-1-expressing EC cells was reduced in *Man1*$^{GT/GT}$ cultures compared with wild types (~30% of total cell population was high PECAM-1$^+$ in wild-type EB cultures compared with only 7% of cells in the *Man1*$^{GT/GT}$ cultures) (Fig. 6C).

Previous evidence suggested that *Man1* regulates cell proliferation. TGFβ1 inhibits fibroblast proliferation, and overexpression of *Man1* decreases the anti-proliferative effect of TGFβ1 (Lin et al., 2005). By contrast, decreased *Man1* expression enhances the anti-proliferative activity of TGFβ1 (Pan et al., 2005). To determine whether disruption of *Man1* increased the sensitivity of cells to the anti-proliferative effect of TGFβ1, we compared cell proliferation in response to TGFβ1 treatment in *Man1*$^{GT/GT}$ and wild-type MEFs (Fig. 6D). Treatment of wild-type MEFs with 1.6 ng/ml of TGFβ1 resulted in a 10% suppression of cell proliferation. By comparison, we also found that TGFβ1 inhibited proliferation of the immortalized mouse endothelial SVEC cell line to a similar extent. By contrast, treatment of *Man1*$^{GT/GT}$ MEFs with TGFβ1 resulted in a significantly increased suppression of cell proliferation by 25%. These results confirm that TGFβ1-mediated inhibition of proliferation is more effective in *Man1*$^{GT/GT}$ cells.

To further characterize the reduction in the proliferation of endothelial cells, the expression of endothelial cell markers and cell cycle mediators was quantitated in the EB explants. Real-time PCR analysis showed that expression of endothelial markers *Flt-1* and *Alk5* (*Tgfbr1* – Mouse Genome Informatics) were both reduced in *Man1*$^{GT/GT}$ cultures (Fig. 6E). Consistent with the observations in the yolk-sac sections (Fig. 5D), the expression of *Acta2* was reduced by 60% relative to wild-type EB explants (Fig. 6E). By contrast, increased expression of the cell cycle inhibitors *p15ink4b* (*Cdkn2b* – Mouse Genome Informatics) and *p27kip1* (*Cdkn1b* – Mouse Genome Informatics) was observed, consistent with the suppression of cell proliferation in the *Man1*$^{GT/GT}$ EB explants. Both *p15ink4b* and *Timp1* are direct transcriptional targets of TGFβ signaling

(Edwards et al., 1987; Hannon and Beach, 1994), and their increased expression suggests that TGFβ signaling is upregulated in the *Man1*$^{GT/GT}$ EB explants.

Enhanced TGFβ signaling in *Man1*$^{GT/GT}$ MEFs

The binding of TGFβ1 to its receptors results in the phosphorylation and subsequent translocation of the receptor-activated SMADs (R-SMADs) from the cytoplasm to the nucleus (Massague and Wotton, 2000). As MAN1 antagonizes BMP and TGFβ1 signaling by interacting with R-SMADs (Hellemans et al., 2004; Lin et al., 2005; Osada et al., 2003; Pan et al., 2005; Raju et al., 2003), we analyzed whether SMAD activity was disrupted in *Man1*$^{GT/GT}$ cells. We examined R-SMAD localization in TGFβ1-treated *Man1*$^{GT/GT}$ MEFs using antibodies to R-SMADs (Fig. 7Aa-i). Untreated wild-type MEFs express equivalent levels of SMAD2/3 in the nucleus and cytoplasm (Fig. 7Aa). Treatment of wild-type MEFs with TGFβ1 resulted in an increase in SMAD2/3 signal in their nuclei (Fig. 7Ab). In the *Man1*$^{GT/GT}$ MEFs, high levels of nuclear SMAD2/3 immunofluorescence were observed in untreated cells (Fig. 7Ac), and this nuclear signal further increased following treatment with TGFβ1 (not shown). Expression of a full-length Flag-tagged MAN1 in wild-type MEFs prevented the nuclear accumulation of SMAD2/3 (Fig. 7Ab,e insets). However, in *Man1*$^{GT/GT}$ MEFs expressing Flag-MAN1, SMAD2/3 was equally distributed between the cytoplasm and nucleus (Fig. 7Ac,f inset), indicating that increased nuclear SMAD accumulation in *Man1*$^{GT/GT}$ MEFs can be reduced by the re-expression of wild-type MAN1.

The increased accumulation of nuclear SMAD2 was quantified by immunoblotting cytoplasmic and nuclear fractions from *Man1*$^{GT/GT}$ and wild-type MEFs (Fig. 7B). Treatment with TGFβ1 resulted in a more robust nuclear localization of SMAD2 in

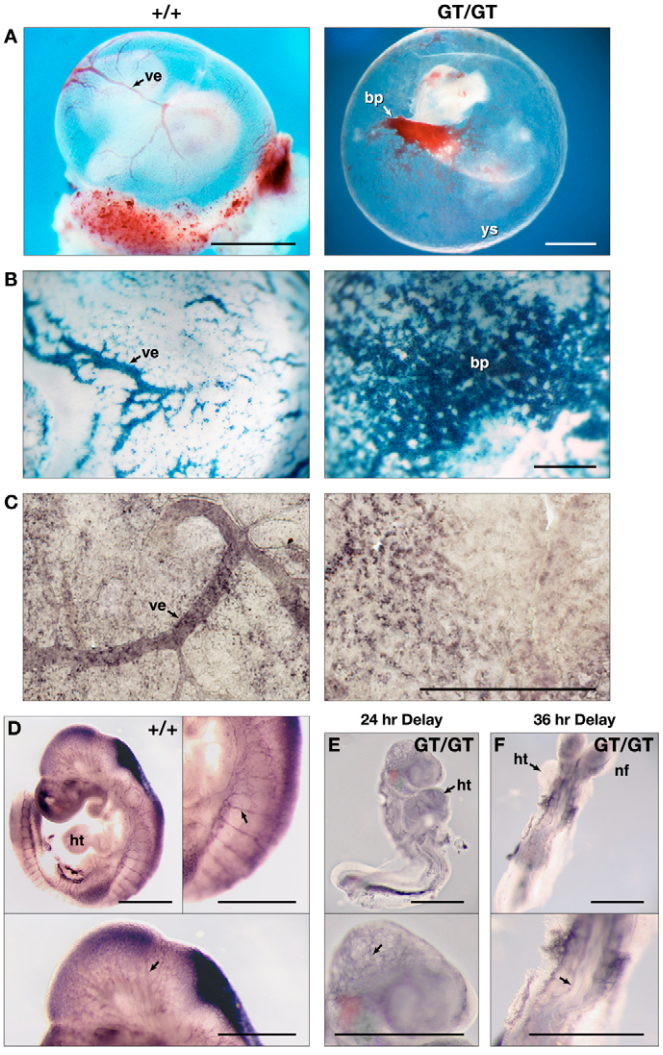

Fig. 4. Abnormal vasculogenesis in *Man1*$^{GT/GT}$ embryos. (**A-C**) Whole-mount views of wild-type (+/+, left) and *Man1*$^{GT/GT}$ (right) yolk sacs. (A) A blood pool formed in the mutant yolk sac at E10.5 instead of the distinct blood vessels in the wild-type at E9.5. (B) Benzidine staining at E9.5 indicates formation of hematopoietic cells within the blood vessels. (C) Whole-mount immunohistochemistry staining at E9.5 with a PECAM-1 antibody labels endothelial cells in the blood vessels. (**D-F**) Whole-mount immunohistochemistry in the embryo proper at E9.5 with a blood vessel marker, FLK-1. Arrows indicate a well-formed vasculature in the wild-type (D) and disorganized vasculature (E) and dorsal aorta (F) in the *Man1*$^{GT/GT}$. (E,F) *Man1*$^{GT/GT}$ embryos appeared to be developmentally delayed by 24-36 hours. bp, blood pool; ht, heart; nf, neural fold; ve, blood vessels; ys, yolk sac. Scale bars: 1 mm.

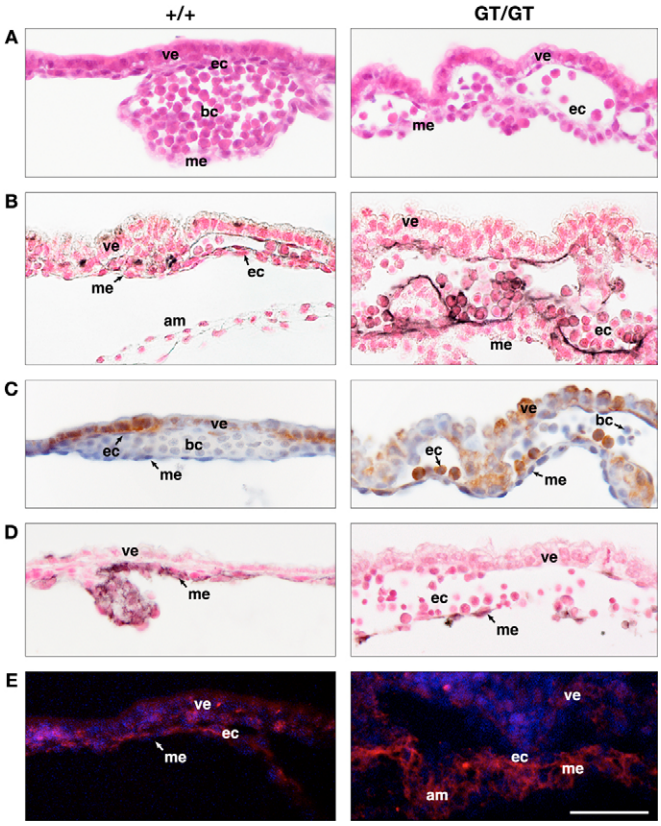

Fig. 5. Expression of endothelial and smooth muscle cell markers in the yolk sacs of *Man1*$^{GT/GT}$ embryos. (**A**) H&E staining of paraffin sections of wild-type (+/+) and *Man1*$^{GT/GT}$ yolk sacs (GT/GT). (**B**) Immunohistochemistry for PECAM-1 reveals disorganized morphology of endothelial cells. Embryos were stained in whole mount followed by paraffin sectioning. (**C**) Immunohistochemistry for FLK-1 showing vascular cell disorganization in the mutant. (**D**) α-smooth muscle actin staining shows a reduction in smooth muscle cells in the mutant. (**E**) Immunofluorescence staining for fibronectin, showing an apparent increase in signal in the mesoderm of the mutant with a reduction of expression in the endoderm. am, amnion; bc, blood cells; ec, endothelial cells; me, mesothelium; ve, visceral endoderm. Scale bar: 50 μm.

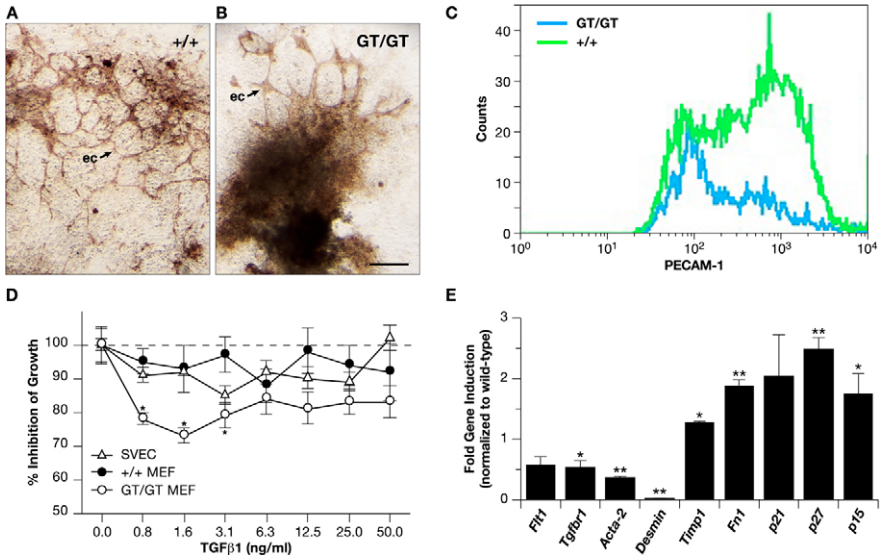

Fig. 6. Endothelial cell proliferation is suppressed in *Man1*$^{GT/GT}$ cells.
(**A**,**B**) Immunohistochemistry of EBs, grown in suspension for 10 days then explanted for 6 days, using an antibody to PECAM-1. (A) Endothelial cells form extensive branches in the wild-type (+/+). (B) The *Man1*$^{GT/GT}$ explants form fewer and less organized branches. (**C**) FACS analysis of PECAM-1^{+} cells isolated from *Man1*$^{GT/GT}$ and wild-type EB explants, showing that in cultures of both genotypes the percentage of PECAM-low expressing cells was similar, but the percentage of PECAM-high expressing cells was strongly reduced in the *Man1*$^{GT/GT}$ cultures. (**D**) TGFβ1 further inhibits cell proliferation in *Man1*$^{GT/GT}$ fibroblasts. Wild-type and *Man1*$^{GT/GT}$ MEFs and SVEC cells were treated with TGFβ1 for 72 hours at the indicated concentrations. Mean±s.e.m. (n=6 wells per treatment). Asterisks indicate statistically significant decrease in the proliferation of *Man1*$^{GT/GT}$ MEFs compared with wild-type and SVEC cells. (**E**) Real-time gene expression analysis of EB explants. EBs were grown in suspension for 14 days then explanted for 4 days. RNA for each data point was derived from >20 EBs and assayed in triplicate. Data are shown as a ratio of *Man1*$^{GT/GT}$ relative to wild type and were normalized to an average of *S18* and *Gapdh*. Mean±s.e.m.; *, P<0.05; **, P<0.005; Student's t-test. Scale bar: 100 μm.

Man1$^{GT/GT}$ MEFs (upper panel). By contrast, in *Man1*$^{GT/GT}$ MEFs expressing a full-length MAN1, the nuclear localization of SMAD2 in *Man1*$^{GT/GT}$ MEFs was significantly reduced (Fig. 7B lower panel).

As TGFβ1 signaling also results in phosphorylation of the R-SMADs, we examined the levels of phosphorylated SMADs1 and 2 (pSMADs1 and 2) in *Man1*$^{GT/GT}$ and wild-type MEFs (Fig. 7C). pSMAD2 levels were higher in untreated *Man1*$^{GT/GT}$ MEFs, compared with wild-type MEFs, and treating *Man1*$^{GT/GT}$ MEFs with TGFβ1 resulted in increased levels of pSMAD2 compared with wild-type MEFs (Fig. 7C lower panel). By contrast, the levels of pSMAD1 were not upregulated in *Man1*$^{GT/GT}$ MEFs (Fig. 7C lower panel).

Transcriptional targets of TGFβ1 signaling are misregulated in *Man1*$^{GT/GT}$ cells

To examine whether the transcription of TGFβ1-regulated genes is affected in *Man1*$^{GT/GT}$ cells, we performed luciferase reporter assays in *Man1*$^{GT/GT}$ and wild-type MEFs (Fig. 7D) transfected with p3TP-Lux (Wrana, 2000). Treatment of *Man1*$^{GT/GT}$ and wild-type MEFs with TGFβ1 for 8 hours resulted in approximately threefold higher levels of normalized luciferase reporter activity than in untreated cultures (Fig. 7D). However, basal luciferase activity was approximately tenfold higher in *Man1*$^{GT/GT}$ MEFs compared with wild types, indicating increased basal levels of R-SMAD-dependent transcription in *Man1*$^{GT/GT}$ MEFs. Together, these data reveal that R-SMAD levels in *Man1*$^{GT/GT}$ cells are not only increased in the nucleus, but also have increased functional activity.

We extended these findings to determine what effect the *Man1*$^{GT/GT}$ mutation has on specific gene expression levels in MEFs. Several known targets of TGFβ1 signaling were analyzed using quantitative real-time PCR in *Man1*$^{GT/GT}$ and wild-type MEFs treated with TGFβ1 for 48 hours (Fig. 7E). Transcript levels of *Pai-1* (*Serpine1* – Mouse Genome Informatics) were upregulated in untreated *Man1*$^{GT/GT}$ MEFs compared with wild-type MEFs and treatment with TGFβ1 resulted in a further ~fivefold increase. Similarly transcript levels of *Timp1* were upregulated in untreated *Man1*$^{GT/GT}$ MEFs compared with wild-type MEFs and were further increased by TGFβ1 treatment. Previous reports using gene profiling of MEFs demonstrated that inhibitor of DNA binding-3 (*Id3*), a target of the BMP signaling pathway, is negatively regulated by TGFβ1 stimulation (Karlsson et al., 2005). *Id3* levels were consistently decreased by the TGFβ1 treatment and showed decreased levels in *Man1*$^{GT/GT}$ MEFs.

Proper yolk-sac formation also requires a balanced deposition in extracellular matrix molecules (Baldwin, 1996). Analysis of fibronectin (Fn; also known as Fn1) expression in yolk-sac sections by immunofluorescence showed that fibronectin levels are increased in the mesoderm but reduced in the endoderm in the *Man1*$^{GT/GT}$ yolk sacs, indicating abnormal extracellular matrix deposition in the *Man1*$^{GT/GT}$ yolk sacs (Fig. 5E). Consistently, we found an upregulation of *Fn* mRNA levels in *Man1*$^{GT/GT}$ EBs (Fig. 6E) and *Man1*$^{GT/GT}$ MEFs (Fig. 7F) and an increase in Fn protein levels in *Man1*$^{GT/GT}$ MEFs (Fig. 7F upper panel). Because the extracellular matrix plays an important role in regulating the proliferation of endothelial cells during lumen formation and blood vessel branching (Baldwin, 1996), increased levels of fibronectin, as well as other extracellular matrix proteins including PAI-1 and TIMP1 in *Man1*$^{GT/GT}$ embryos, may have a direct impact on EC proliferation and migration, resulting in defective vasculogenesis. In addition, expression of cell cycle regulator *p21waf1* (*Cdkn1a* – Mouse Genome Informatics) was increased in *Man1*$^{GT/GT}$ MEFs (Fig. 7F, lower panel), indicating that increased TGFβ1 signaling and activation of cell cycle regulators may contribute to the decreased proliferation of ECs in *Man1*$^{GT/GT}$ embryos.

DISCUSSION

Requirement of a functional *Man1* by the embryonic yolk-sac mesoderm

During mammalian embryogenesis, one of the first tissues formed after embryo implantation is the vascular system. This tissue is essential to sustain the growth and differentiation of the other embryonic tissues, to supply them with nutrients and oxygen, as well

as to remove their metabolic waste products. Considerable information already exists as to which growth factors regulate the development of the vascular system in mouse embryos, and among these factors the TGFβ signaling pathway has a central role (Mummery, 2001; Rossant and Howard, 2002).

The TGFβ superfamily of growth factors consists of a multitude of ligands, receptors and transcription factors, as well as other less well-defined proteins regulating the activation of the pathways. Such complexity reflects the many proliferative, differentiative and physiological functions regulated by the TGFβ superfamily (Feng and Derynck, 2005; Massague et al., 2005). One of the more recently identified factors implicated in regulating TGFβ signaling is the nuclear-envelope-associated protein MAN1. Recent studies showed that the nucleoplasmic RRM domain at the C-terminus of MAN1 binds, and seemingly sequesters, SMADs1-3 to the nuclear envelope. Such sequestration regulates SMAD nuclear translocation and transcriptional activity, by an as yet undefined mechanism (Lin et al., 2005; Pan et al., 2005). Here we show that disruption of the *Man1* gene leads to the death of homozygous mouse embryos around the time vascularization commences, probably by perturbing TGFβ signaling in the yolk-sac mesoderm.

The *Man1*$^{GT/GT}$ phenotype is mediated by defective TGFβ signaling

In the *Man1*$^{GT/GT}$ embryos, abnormal yolk-sac vasculogenesis is phenotypically similar to previously reported defects arising from mutations in receptors, ligands and other components of the TGFβ signaling pathway (Agah et al., 2000; Dickson et al., 1995; Larsson et al., 2001; Oshima et al., 1996). Yolk-sac vasculogenesis consists of a proliferative activation state and a final resolution state, which are mediated by the coordinate activation by TGFβ of two parallel receptor-mediated cellular pathways (Oh et al., 2000). TGFβ1 acting

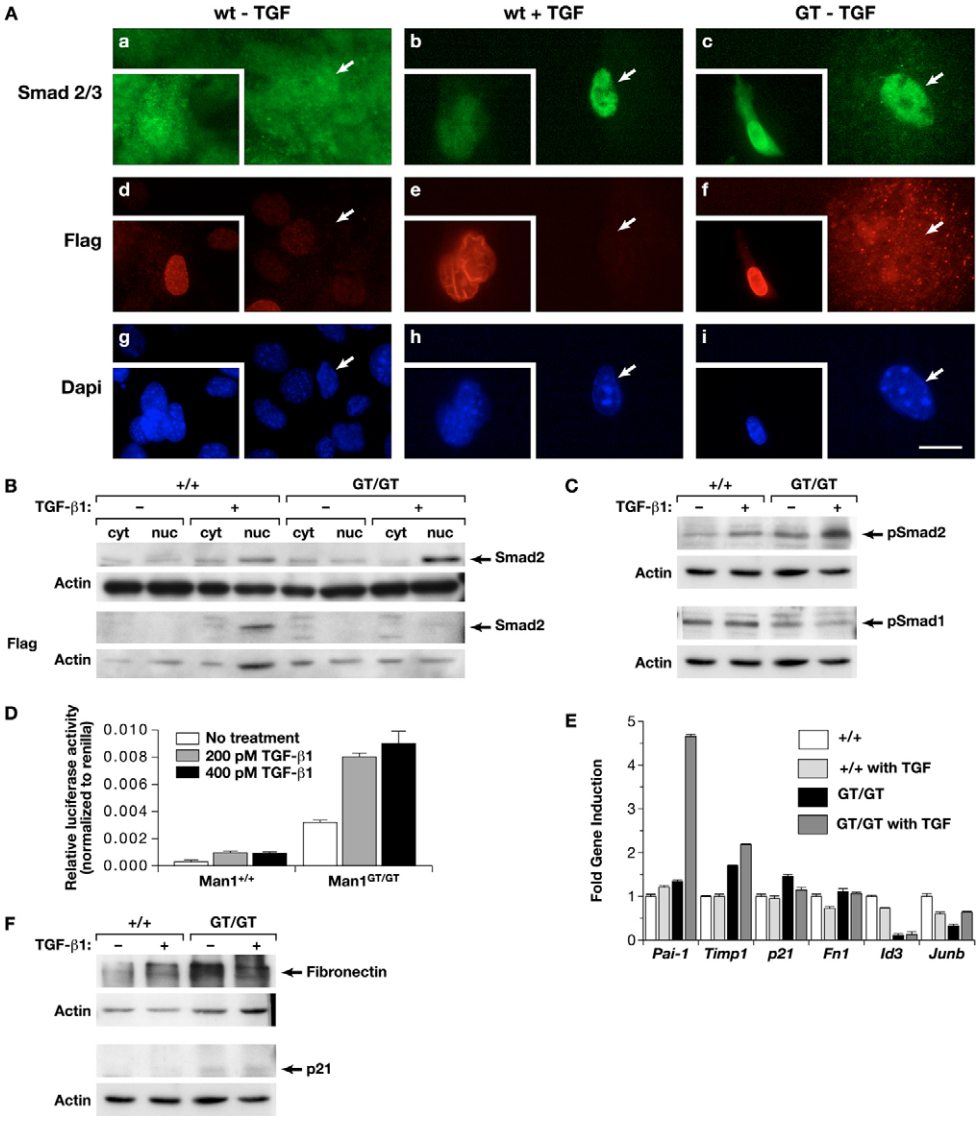

Fig. 7. Upregulation of TGFβ signaling in *Man1*$^{GT/GT}$ MEFs. (**A a-i**) Immunofluorescence staining of TGFβ-treated or untreated wild-type (wt) and *Man1*$^{GT/GT}$ MEFs with an antibody to SMAD2/3 (a-c). Cells were infected with a Flag-tagged MAN1 retroviral vector; Flag-positive cells are shown in insets, Flag-negative cells are indicated by arrows (d-f). Dapi was used to show nuclei (g-i). (a) In unstimulated MEFs SMADs2/3 are distributed between the nuclei and cytoplasm. (b) Following treatment with TGFβ1 SMADs2/3 accumulate in the nucleus. (c) In *Man1*$^{GT/GT}$ MEFs, SMAD2 shows a strong nuclear localization in the absence of TGFβ1 treatment. (b,e) In wild-type MEFs, overexpression of MAN1 reduces SMADs2/3 accumulation (inset). (c,f) In the *Man1*$^{GT/GT}$ MEFs, MAN1 similarly redistributes SMADs2/3 to the cytoplasm (inset). Scale bar: 20 μm. (**B**) Western blot of SMAD2 concentrations in the nucleus and cytoplasm. Upper panel: following TGFβ1 treatment, wild-type (+/+) and *Man1*$^{GT/GT}$ (GT/GT) MEFs were fractionated into nuclear and cytoplasmic extracts and immunoblotted with an antibody to SMAD2. Both TGFβ1 untreated and treated *Man1*$^{GT/GT}$ cells show enhanced nuclear accumulation of SMAD2. Bottom panel: immunoblot of nuclear and cytoplasmic fractions prepared from *Man1*$^{GT/GT}$ and wild-type MEFs expressing Flag-MAN1 showing a marked reduction in the nuclear accumulation of SMAD2. (**C**) Western blot of MEF whole cell lysates with antibodies to SMAD2 (upper) and SMAD1 (lower). SMAD2, but not SMAD1 is hyperphosphorylated in *Man1*$^{GT/GT}$ MEFs following treatment with TGFβ1. (**D**) *Man1*$^{GT/GT}$ MEFs show higher levels of both basal and stimulated SMAD transcriptional activity. *Man1*$^{GT/GT}$ and wild-type MEFs were transfected with a TGFβ-responsive reporter plasmid p3TP-Lux and co-transfected with pTK-RL. Transfected cells were stimulated with indicated concentrations of TGFβ1 and analyzed for luciferase activity. Mean±s.e.m.; n=3. (**E**) Real-time PCR analysis of TGFβ target genes. MEFs were treated with TGFβ1 and quantitative PCR analysis performed on duplicate extracts. Means±s.e.m. are indicated. (**F**) Western analysis shows upregulated fibronectin (upper) and *p21waf1* (lower) protein levels in TGFβ1 treated *Man1*$^{GT/GT}$ MEFs. Actin was used as a loading control.

through the ALK1 receptor and SMADs1/5/8, mediates the activation state leading to proliferation of endothelial cells as well as recruitment of smooth muscle cells; whereas TGFβ1 acting through the ALK5 receptor and SMADs2/3, inhibits the proliferation of endothelial cells (Bertolino et al., 2005; Goumans et al., 2002; Pepper, 1997). Supportive of this model, functional deletion of *Alk5* in mice leads to defects both in hematopoiesis and vasculogenesis and death around day E10.5. Endothelial cells derived from the deficient animals are over-proliferative and show reduced levels of *Fn* in response to TGFβ1 (Larsson et al., 2001). However, mice deficient in *Alk1* (*Acvrl1* – Mouse Genome Informatics) also develop defects in angiogenesis and show upregulation of the ALK5-regulated *Pai-1* (Oh et al., 2000). Comparably, cells overexpressing *Alk5* show decreased proliferation, downregulation of inhibitory factor *Id1* and upregulation of *Pai-1* (Goumans et al., 2002). Finally, disruption of *Endoglin*, a component of the TGFβ1 receptor complex that antagonizes TGFβ signaling through the ALK5 receptor, also results in defective angiogenesis (Arthur et al., 2000; Li et al., 1999; van den Driesche et al., 2003).

Several lines of evidence from our studies suggest that the defect in vascularization in $Man1^{GT/GT}$ yolk sacs is preferentially mediated through an overactivated ALK5 pathway. Results from the western analysis showed that ALK5-responsive SMAD2 and not ALK1-responsive SMAD1 is hyperphosphorylated and more concentrated in the nucleus. In $Man1^{GT/GT}$ MEFs and EBs, proliferation of ECs and VSMCs is reduced, suggesting that vascularization in $Man1^{GT/GT}$ yolk sacs is compromised due to insufficient numbers of cells being available to remodel the existing capillary plexus. This reduction in cell number correlated with upregulation in the expression of the cell cycle inhibitors *p15ink4b*, *p21waf1* and *p27kip1*. In addition, increased ECM deposition (Goumans et al., 1999), together with increased PAI-1 inhibit EC migration and angiogenic branching (Ignotz and Massague, 1986; McIlroy et al., 2006). Thus, increased Fn and *Pai-1* levels in $Man1^{GT/GT}$ embryos may have also exacerbated the effects on EC proliferation and contributed to defective vasculogenesis in $Man1^{GT/GT}$ yolk sacs.

During the review process of this paper, a complementary study of the $Man1^{GT/GT}$ phenotype was published (Ishimura et al., 2006). Consistent with our findings, the authors demonstrated elevated nuclear levels of SMADs2/3, as well as increased ECM deposition in the $Man1^{GT/GT}$ mice. Interestingly, the authors attribute the increase in ECM due to apoptosis, not cell proliferation, as suggested by an apparent lack of increased phosphohistone 3 signal in the embryo sections. Although not inconsistent with this observation, our conclusion from the cellular proliferation analysis and upregulation of cell cycle inhibitor proteins, suggests that decreased proliferation does play a role in the vascular defect.

MAN1 regulates nuclear localization and phosphorylation of SMADs

R-SMADs are normally in equilibrium between the cytoplasm and the nucleus (Risau and Flamme, 1995; Xiao et al., 2001; Xu et al., 2002). Stimulation by TGFβ1 increases the levels of phosphorylated R-SMADs in the nucleus. Activated R-SMADs are subject to negative regulation by nuclear factors such as c-Ski, SARA and SMURFs (Massague and Chen, 2000). Gating the entry and exit of R-SMADs into the nucleus is another means of regulating a balance of cellular response to TGFβ stimulation (Luo, 2004).

The RRM domain of MAN1 physically interacts with R-SMADs, so regulating SMAD activity (Lin et al., 2005; Osada et al., 2003; Pan et al., 2005). We demonstrated that disruption of MAN1 results in enhanced SMAD2/3 nuclear localization and transcriptional activity, leading to the altered expression of genes regulated by TGFβ1. Although the nucleoplasmic localization of pSMAD2 was increased in $Man1^{GT/GT}$ MEFs in the absence of TGFβ1 addition, this was probably due to stimulation by endogenous TGFβ/BMPs in the serum in which the cells were cultured (Ying et al., 2003). However, treatment of $Man1^{GT/GT}$ MEFs with TGFβ1 further increased the nuclear concentration and activity of R-SMADs, suggesting that MAN1 regulates the entry/exit of SMADs in the nucleus. Our observations also suggest that MAN1 regulates the nuclear localization and transcriptional activity of SMADs by affecting SMAD phosphorylation. Although MAN1 has not been shown to possess any intrinsic phosphatase activity, the C-terminal domain may act as a scaffold or binding site that brings phosphorylated SMADs into an association with SMAD phosphatases (Chen et al., 2006; Knockaert et al., 2006; Lin et al., 2006). A similar role for the nuclear lamina affecting the phosphorylation state of SMADs was recently proposed, as loss of the A-type lamins may affect TGFβ1-mediated SMAD phosphorylation by regulating protein phosphatase 2A (Van Berlo et al., 2005). Whether the lamin A-mediated pathway is independent of MAN1 in regulating SMAD phosphorylation and activity remains to be demonstrated.

Role of MAN1 may differ between species

Functional analysis of MAN1 in different species has revealed differing roles, possibly reflecting tissue specificity (Hellemans et al., 2004; Osada et al., 2003). In *Xenopus* embryos, a reduction in XMAN1 disrupted the formation of anterior neural structures, suggesting that in XMAN1 antagonizes BMP signaling (Osada et al., 2003). Formation of the neural crest and anterior neural structures appeared to be overtly normal in $Man1^{GT/GT}$ embryos before their death. However, as *Man1* transcripts are abundantly expressed in the adult brain, we cannot rule out that *Man1* may still play an undefined role in later development of the nervous system. In humans, loss-of-function mutations in *MAN1* result in osteopoikilosis, melorheostosis and Buschke-Ollendorf syndrome (Hellemans et al., 2004). Although we performed X-ray scans on the bones from adult $Man1^{GT/+}$ mice, we did not detect any evidence of hyperostotic lesions, and the bone density in $Man1^{GT/+}$ mice was similar to that of wild-type mice (data not shown). It is unclear whether failure to detect bone defects in the heterozygous mice is due to possible differences in the age of onset of lesions between humans and mice, or due to differences between the types of mutation between the human gene and the gene-trap. As the N-terminal sequence of MAN1 is still present in $Man1^{GT}$ mice, and targeting to the NE is undisturbed, it is possible that the remaining sequence, including the LEM domain, may prevent $Man1^{GT/GT}$ embryos from developing additional phenotypes.

The nuclear envelope/lamina in development

Our findings and other recent evidence strengthens the notion that the NE/lamina is an important nuclear compartment regulating chromatin organization and gene expression. Studies in yeast revealed the importance of the NE in gene silencing and telomere function (Taddei et al., 2004). Recent studies have shown that the lamina may be important for the sequestration, and to some extent function, of crucial regulatory factors such as the c-Fos and Retinoblastoma (Rb) proto-oncogenes (Ivorra et al., 2006; Markiewicz et al., 2002; Melcon et al., 2006). Also, silencing in the expression of tissue-specific transcription factors such as MyoD, and the activity of the chromatin insulator *gypsy*, is associated with their localization to the nuclear periphery and lamina, respectively (Capelson and Corces, 2005; Lee et al., 2006). In this capacity,

MAN1, a transmembrane protein of the INM that is differentially expressed during development and in adult tissues, may act as a scaffold protein regulating SMAD phosphorylation, localization and activity. The NE and lamina may therefore have many additional, as yet undiscovered, roles in regulating cell differentiation and function during development.

This research was supported by the Intramural Research Program of the NIH, National Cancer Institute, Center for Cancer Research. We wish to thank Amanda Boyce and Rocky Tuan for X-ray analysis of the mice; Howard Worman for providing the MAN1 cDNA; Steve Young and Jonathan Cohen for advice; and Richard Frederickson for preparation of the figures.

References

Abbondanzo, S. J., Gadi, I. and Stewart, C. L. (1993). Derivation of embryonic stem cell lines. *Meth. Enzymol.* **225**, 803-823.

Agah, R., Prasad, K. S., Linnemann, R., Firpo, M. T., Quertermous, T. and Dichek, D. A. (2000). Cardiovascular overexpression of transforming growth factor-beta(1) causes abnormal yolk sac vasculogenesis and early embryonic death. *Circ. Res.* **86**, 1024-1030.

Arthur, H. M., Ure, J., Smith, A. J., Renforth, G., Wilson, D. I., Torsney, E., Charlton, R., Parums, D. V., Jowett, T., Marchuk, D. A. et al. (2000). Endoglin, an ancillary TGFbeta receptor, is required for extraembryonic angiogenesis and plays a key role in heart development. *Dev. Biol.* **217**, 42-53.

Baldwin, H. S. (1996). Early embryonic vascular development. *Cardiovasc. Res.* **31**, E34-E45.

Baron, M. H. (2003). Embryonic origins of mammalian hematopoiesis. *Exp. Hematol.* **31**, 1160-1169.

Bertolino, P., Deckers, M., Lebrin, F. and ten Dijke, P. (2005). Transforming growth factor-beta signal transduction in angiogenesis and vascular disorders. *Chest* **128**, 585S-590S.

Burke, B. and Stewart, C. L. (2002). Life at the edge: the nuclear envelope and human disease. *Nat. Rev. Mol. Cell Biol.* **3**, 575-585.

Byrd, N., Becker, S., Maye, P., Narasimhaiah, R., St-Jacques, B., Zhang, X., McMahon, J., McMahon, A. and Grabel, L. (2002). Hedgehog is required for murine yolk sac angiogenesis. *Development* **129**, 361-372.

Cai, M., Huang, Y., Ghirlando, R., Wilson, K. L., Craigie, R. and Clore, G. M. (2001). Solution structure of the constant region of nuclear envelope protein LAP2 reveals two LEM-domain structures: one binds BAF and the other binds DNA. *EMBO J.* **20**, 4399-4407.

Capelson, M. and Corces, V. G. (2005). The ubiquitin ligase dTopors directs the nuclear organization of a chromatin insulator. *Mol. Cell* **20**, 105-116.

Chen, H. B., Shen, J., Ip, Y. T. and Xu, L. (2006). Identification of phosphatases for Smad in the BMP/DPP pathway. *Genes Dev.* **20**, 648-653.

Dickson, M. C., Martin, J. S., Cousins, F. M., Kulkarni, A. B., Karlsson, S. and Akhurst, R. J. (1995). Defective haematopoiesis and vasculogenesis in transforming growth factor-beta 1 knock out mice. *Development* **121**, 1845-1854.

Edwards, D. R., Murphy, G., Reynolds, J. J., Whitham, S. E., Docherty, A. J., Angel, P. and Heath, J. K. (1987). Transforming growth factor beta modulates the expression of collagenase and metalloproteinase inhibitor. *EMBO J.* **6**, 1899-1904.

Escalante-Alcalde, D., Hernandez, L., Le Stunff, H., Maeda, R., Lee, H. S., Jr, Gang, C., Sciorra, V. A., Daar, I., Spiegel, S., Morris, A. J. et al. (2003). The lipid phosphatase LPP3 regulates extra-embryonic vasculogenesis and axis patterning. *Development* **130**, 4623-4637.

Feinberg, M. W., Watanabe, M., Lebedeva, M. A., Depina, A. S., Hanai, J., Mammoto, T., Frederick, J. P., Wang, X. F., Sukhatme, V. P. and Jain, M. K. (2004). Transforming growth factor-beta1 inhibition of vascular smooth muscle cell activation is mediated via Smad3. *J. Biol. Chem.* **279**, 16388-16393.

Feng, X. H. and Derynck, R. (2005). Specificity and versatility in tgf-beta signaling through Smads. *Annu. Rev. Cell Dev. Biol.* **21**, 659-693.

Goumans, M. J. and Mummery, C. (2000). Functional analysis of the TGFbeta receptor/Smad pathway through gene ablation in mice. *Int. J. Dev. Biol.* **44**, 253-265.

Goumans, M. J., Zwijsen, A., van Rooijen, M. A., Huylebroeck, D., Roelen, B. A. and Mummery, C. L. (1999). Transforming growth factor-beta signalling in extraembryonic mesoderm is required for yolk sac vasculogenesis in mice. *Development* **126**, 3473-3483.

Goumans, M. J., Valdimarsdottir, G., Itoh, S., Rosendahl, A., Sideras, P. and ten Dijke, P. (2002). Balancing the activation state of the endothelium via two distinct TGF-beta type I receptors. *EMBO J.* **21**, 1743-1753.

Gruenbaum, Y., Margalit, A., Goldman, R. D., Shumaker, D. K. and Wilson, K. L. (2005). The nuclear lamina comes of age. *Nat. Rev. Mol. Cell Biol.* **6**, 21-31.

Hannon, G. J. and Beach, D. (1994). p15INK4B is a potential effector of TGF-beta-induced cell cycle arrest. *Nature* **371**, 257-261.

Hellemans, J., Preobrazhenska, O., Willaert, A., Debeer, P., Verdonk, P. C., Costa, T., Janssens, K., Menten, B., Van Roy, N., Vermeulen, S. J. et al. (2004). Loss-of-function mutations in LEMD3 result in osteopoikilosis, Buschke-Ollendorff syndrome and melorheostosis. *Nat. Genet.* **36**, 1213-1218.

Hellemans, J., Debeer, P., Wright, M., Janecke, A., Kjaer, K. W., Verdonk, P. C., Savarirayan, R., Basel, L., Moss, C., Roth, J. et al. (2006). Germline LEMD3 mutations are rare in sporadic patients with isolated melorheostosis. *Hum. Mutat.* **27**, 290.

Ignotz, R. A. and Massague, J. (1986). Transforming growth factor-beta stimulates the expression of fibronectin and collagen and their incorporation into the extracellular matrix. *J. Biol. Chem.* **261**, 4337-4345.

Ishimura, A., Ng, J. K., Taira, M., Young, S. G. and Osada, S. (2006). Man1, an inner nuclear membrane protein, regulates vascular remodeling by modulating transforming growth factor beta signaling. *Development* **133**, 3919-3928.

Ivorra, C., Kubicek, M., Gonzalez, J. M., Sanz-Gonzalez, S. M., Alvarez-Barrientos, A., O'Connor, J. E., Burke, B. and Andres, V. (2006). A mechanism of AP-1 suppression through interaction of c-Fos with lamin A/C. *Genes Dev.* **20**, 307-320.

Karlsson, G., Liu, Y., Larsson, J., Goumans, M. J., Lee, J. S., Thorgeirsson, S. S., Ringner, M. and Karlsson, S. (2005). Gene expression profiling demonstrates that TGF-beta1 signals exclusively through receptor complexes involving Alk5 and identifies targets of TGF-beta signaling. *Physiol. Genomics* **21**, 396-403.

Knockaert, M., Sapkota, G., Alarcon, C., Massague, J. and Brivanlou, A. H. (2006). Unique players in the BMP pathway: small C-terminal domain phosphatases dephosphorylate Smad1 to attenuate BMP signaling. *Proc. Natl. Acad. Sci. USA* **103**, 11940-11945.

Laguri, C., Gilquin, B., Wolff, N., Romi-Lebrun, R., Courchay, K., Callebaut, I., Worman, H. J. and Zinn-Justin, S. (2001). Structural characterization of the LEM motif common to three human inner nuclear membrane proteins. *Structure* **9**, 503-511.

Larsson, J., Goumans, M. J., Sjostrand, L. J., van Rooijen, M. A., Ward, D., Leveen, P., Xu, X., ten Dijke, P., Mummery, C. L. and Karlsson, S. (2001). Abnormal angiogenesis but intact hematopoietic potential in TGF-beta type I receptor-deficient mice. *EMBO J.* **20**, 1663-1673.

Lee, H., Quinn, J. C., Prasanth, K. V., Swiss, V. A., Economides, K. D., Camacho, M. M., Spector, D. L. and Abate-Shen, C. (2006). PIAS1 confers DNA-binding specificity on the Msx1 homeoprotein. *Genes Dev.* **20**, 784-794.

Lee, K. K. and Wilson, K. L. (2004). All in the family: evidence for four new LEM-domain proteins Lem2 (NET-25), Lem3, Lem4 and Lem5 in the human genome. *Symp. Soc. Exp. Biol.* **2004**, 329-339.

Levenberg, S., Golub, J. S., Amit, M., Itskovitz-Eldor, J. and Langer, R. (2002). Endothelial cells derived from human embryonic stem cells. *Proc. Natl. Acad. Sci. USA* **99**, 4391-4396.

Li, D. Y., Sorensen, L. K., Brooke, B. S., Urness, L. D., Davis, E. C., Taylor, D. G., Boak, B. B. and Wendel, D. P. (1999). Defective angiogenesis in mice lacking endoglin. *Science* **284**, 1534-1537.

Lin, F., Blake, D. L., Callebaut, I., Skerjanc, I. S., Holmer, L., McBurney, M. W., Paulin-Levasseur, M. and Worman, H. J. (2000). MAN1, an inner nuclear membrane protein that shares the LEM domain with lamina-associated polypeptide 2 and emerin. *J. Biol. Chem.* **275**, 4840-4847.

Lin, F., Morrison, J. M., Wu, W. and Worman, H. J. (2005). MAN1, an integral protein of the inner nuclear membrane, binds Smad2 and Smad3 and antagonizes transforming growth factor-beta signaling. *Hum. Mol. Genet.* **14**, 437-445.

Lin, X., Duan, X., Liang, Y. Y., Su, Y., Wrighton, K. H., Long, J., Hu, M., Davis, C. M., Wang, J., Brunicardi, F. C. et al. (2006). PPM1A functions as a Smad phosphatase to terminate TGFbeta signaling. *Cell* **125**, 915-928.

Luo, K. (2004). Ski and SnoN: negative regulators of TGF-beta signaling. *Curr. Opin. Genet. Dev.* **14**, 65-70.

Markiewicz, E., Dechat, T., Foisner, R., Quinlan, R. A. and Hutchison, C. J. (2002). Lamin A/C binding protein LAP2alpha is required for nuclear anchorage of retinoblastoma protein. *Mol. Biol. Cell* **13**, 4401-4413.

Massague, J. and Chen, Y. G. (2000). Controlling TGF-beta signaling. *Genes Dev.* **14**, 627-644.

Massague, J. and Wotton, D. (2000). Transcriptional control by the TGF-beta/Smad signaling system. *EMBO J.* **19**, 1745-1754.

Massague, J., Seoane, J. and Wotton, D. (2005). Smad transcription factors. *Genes Dev.* **19**, 2783-2810.

McIlroy, M., O'Rourke, M., McKeown, S. R., Hirst, D. G. and Robson, T. (2006). Pericytes influence endothelial cell growth characteristics: role of plasminogen activator inhibitor type 1 (PAI-1). *Cardiovasc. Res.* **69**, 207-217.

Melcon, G., Kozlov, S., Cutler, D. A., Sullivan, T., Hernandez, L., Zhao, P., Mitchell, S., Nader, G., Bakay, M., Rottman, J. N. et al. (2006). Loss of emerin at the nuclear envelope disrupts the Rb1/E2F and MyoD pathways during muscle regeneration. *Hum. Mol. Genet.* **15**, 637-651.

Morris, G. E. (2004). Protein interactions, right or wrong, in Emery-Dreifuss muscular dystrophy. *Symp. Soc. Exp. Biol.* **2004**, 57-68.

Mummery, C. L. (2001). Transforming growth factor beta and mouse development. *Microsc. Res. Tech.* **52**, 374-386.

O'Connell, K. A. and Edidin, M. (1990). A mouse lymphoid endothelial cell line

immortalized by simian virus 40 binds lymphocytes and retains functional characteristics of normal endothelial cells. *J. Immunol.* **144**, 521-525.
Oh, S. P., Seki, T., Goss, K. A., Imamura, T., Yi, Y., Donahoe, P. K., Li, L., Miyazono, K., ten Dijke, P., Kim, S. et al. (2000). Activin receptor-like kinase 1 modulates transforming growth factor-beta 1 signaling in the regulation of angiogenesis. *Proc. Natl. Acad. Sci. USA* **97**, 2626-2631.
Orkin, S. H., Harosi, F. I. and Leder, P. (1975). Differentiation in erythroleukemic cells and their somatic hybrids. *Proc. Natl. Acad. Sci. USA* **72**, 98-102.
Osada, S., Ohmori, S. Y. and Taira, M. (2003). XMAN1, an inner nuclear membrane protein, antagonizes BMP signaling by interacting with Smad1 in Xenopus embryos. *Development* **130**, 1783-1794.
Oshima, M., Oshima, H. and Taketo, M. M. (1996). TGF-beta receptor type II deficiency results in defects of yolk sac hematopoiesis and vasculogenesis. *Dev. Biol.* **179**, 297-302.
Pan, D., Estevez-Salmeron, L. D., Stroschein, S. L., Zhu, X., He, J., Zhou, S. and Luo, K. (2005). The integral inner nuclear membrane protein MAN1 physically interacts with the R-Smad proteins to repress signaling by the transforming growth factor-{beta} superfamily of cytokines. *J. Biol. Chem.* **280**, 15992-16001.
Pepper, M. S. (1997). Transforming growth factor-beta: vasculogenesis, angiogenesis, and vessel wall integrity. *Cytokine Growth Factor Rev.* **8**, 21-43.
Raju, G. P., Dimova, N., Klein, P. S. and Huang, H. C. (2003). SANE, a novel LEM domain protein, regulates bone morphogenetic protein signaling through interaction with Smad1. *J. Biol. Chem.* **278**, 428-437.
Risau, W. and Flamme, I. (1995). Vasculogenesis. *Annu. Rev. Cell Dev. Biol.* **11**, 73-91.
Rossant, J. and Cross, J. C. (2001). Placental development: lessons from mouse mutants. *Nat. Rev. Genet.* **2**, 538-548.
Rossant, J. and Howard, L. (2002). Signaling pathways in vascular development. *Annu. Rev. Cell Dev. Biol.* **18**, 541-573.
Schirmer, E. C., Florens, L., Guan, T., Yates, J. R., 3rd and Gerace, L. (2003). Nuclear membrane proteins with potential disease links found by subtractive proteomics. *Science* **301**, 1380-1382.
Schlaeger, T. M., Qin, Y., Fujiwara, Y., Magram, J. and Sato, T. N. (1995). Vascular endothelial cell lineage-specific promoter in transgenic mice. *Development* **121**, 1089-1098.
Skarnes, W. C. (1990). Entrapment vectors: a new tool for mammalian genetics. *Biotechnology N. Y.* **8**, 827-831.
Stewart, C. L. (1993). Production of chimeras between embryonic stem cells and embryos. *Meth. Enzymol.* **225**, 823-855.
Stewart, C. L., Abbondanzo, S. J. and Cullinan, E. B. (1995). [Regulation by maternally derived cytokines of pre-implantation development and uterine receptiveness]. *Contracept. Fertil. Sex.* **23**, 555-561.
Taddei, A., Hediger, F., Neumann, F. R. and Gasser, S. M. (2004). The function of nuclear architecture: a genetic approach. *Annu. Rev. Genet.* **38**, 305-345.
Taylor, M. R., Slavov, D., Gajewski, A., Vlcek, S., Ku, L., Fain, P. R., Carniel, E., Di Lenarda, A., Sinagra, G., Boucek, M. M. et al. (2005). Thymopoietin (lamina-associated polypeptide 2) gene mutation associated with dilated cardiomyopathy. *Hum. Mutat.* **26**, 566-574.
Van Berlo, J. H., Voncken, J. W., Kubben, N., Broers, J. L., Duisters, R., van Leeuwen, R. E., Crijns, H. J., Ramaekers, F. C., Hutchison, C. J. and Pinto, Y. M. (2005). A-type lamins are essential for TGF-beta1 induced PP2A to dephosphorylate transcription factors. *Hum. Mol. Genet.* **14**, 2839-2849.
van den Driesche, S., Mummery, C. L. and Westermann, C. J. (2003). Hereditary hemorrhagic telangiectasia: an update on transforming growth factor beta signaling in vasculogenesis and angiogenesis. *Cardiovasc. Res.* **58**, 20-31.
Wolff, N., Gilquin, B., Courchay, K., Callebaut, I., Worman, H. J. and Zinn-Justin, S. (2001). Structural analysis of emerin, an inner nuclear membrane protein mutated in X-linked Emery-Dreifuss muscular dystrophy. *FEBS Lett.* **501**, 171-176.
Worman, H. J. (2005). Components of the nuclear envelope and their role in human disease. *Novartis Found. Symp.* **264**, 35-42; discussion 42-50, 227-230.
Wrana, J. L. (2000). Regulation of Smad activity. *Cell* **100**, 189-192.
Xiao, Z., Watson, N., Rodriguez, C. and Lodish, H. F. (2001). Nucleocytoplasmic shuttling of Smad1 conferred by its nuclear localization and nuclear export signals. *J. Biol. Chem.* **276**, 39404-39410.
Xu, L., Kang, Y., Col, S. and Massague, J. (2002). Smad2 nucleocytoplasmic shuttling by nucleoporins CAN/Nup214 and Nup153 feeds TGFbeta signaling complexes in the cytoplasm and nucleus. *Mol. Cell* **10**, 271-282.
Ying, Q. L., Nichols, J., Chambers, I. and Smith, A. (2003). BMP induction of Id proteins suppresses differentiation and sustains embryonic stem cell self-renewal in collaboration with STAT3. *Cell* **115**, 281-292.
Zhu, J. Y., Abate, M., Rice, P. W. and Cole, C. N. (1991). The ability of simian virus 40 large T antigen to immortalize primary mouse embryo fibroblasts cosegregates with its ability to bind to p53. *J. Virol.* **65**, 6872-6880.
Zwijsen, A., Goumans, M. J., Lawson, K. A., Van Rooijen, M. A. and Mummery, C. L. (1999). Ectopic expression of the transforming growth factor beta type II receptor disrupts mesoderm organisation during mouse gastrulation. *Dev. Dyn.* **214**, 141-151.